Kidney Diseases

Research Article

Kidney Dis 2025;11:11–24
DOI: 10.1159/000542471

Received: April 30, 2024
Accepted: October 30, 2024
Published online: November 21, 2024

Neutrophil Extracellular Traps Drive Kidney Stone Formation

Zhiming Yang[a, b] Xiong Chen[a, b] Guannan Qi[a, b] Jie Gu[a, b] Zheng Liu[a, b] Xiaobo Zhang[a, b, c]

[a]Department of Geriatric Urology, Xiangya International Medical Center, Xiangya Hospital, Central South University, Changsha, PR China; [b]National Clinical Research Center for Geriatric Disorders, Xiangya Hospital, Central South University, Changsha, PR China; [c]Urolithiasis Institute of Central South University, Changsha, PR China

Keywords
Neutrophil extracellular traps · Kidney stones · Apoptosis · Calcium deposits · Renal tubular injury

Abstract
Introduction: This study aims to explore the contribution of neutrophil extracellular traps (NETs) to kidney stones. ***Methods:*** The microarray data from GSE73680 and bioinformatic analysis were applied to identify differentially expressed genes in patients with kidney stones. A rat model of kidney stones was established through ethylene glycol and ammonium chloride administration. The plasma was collected for examining cf-DNA, DNase I, MPO-DNA, H3Cit and NE. Superoxide dismutase, malondialdehyde, creatinine, blood urea nitrogen, and calcium were examined through biochemical analysis. MPO, H3Cit, and NE in kidney tissues were detected via immunofluorescence staining. Cell apoptosis was evaluated through TUNEL assays. HE, Periodic Acid-Schiff and Von Kossa staining were applied to determine histological structure, calcium deposits and stone formation in the kidneys. Neutrophil elastase inhibitor Sivelestat (SIVE) was administrated for NET suppression in rats. ***Results:*** A total of 403 differentially expressed genes including 270 upregulated and 133 downregulated genes were identified between renal papillary tissues with Randall's plaque and normal tissues. Gene ontology enrichment, KEGG pathway and protein-protein interaction network analysis of these dysregulated genes were performed. Moreover, increased NET markers including cf-DNA, DNase I, MPO-DNA, H3Cit and NE and calcium deposits were observed in patients with kidney stones. Subsequently, we established a rat model of kidney stones. We found that NET formation was significantly elevated in kidney stone rats, and renal tubular injury and apoptotic cells were enhanced as kidney stones developed. Strikingly, we found that suppression of NETs via SIVE could significantly reduce calcium deposits and apoptotic cells and alleviate tubular injury, thus improving kidney function. ***Conclusion:*** NETs drive the formation of kidney stones, thus aggravating kidney injury. Our study identifies NETs as a potential diagnostic and therapeutic biomarker for nephrolithiasis.

© 2024 The Author(s).
Published by S. Karger AG, Basel

Introduction

Kidney stones, also known as urolithiasis or nephrolithiasis, are mineral deposits that form in the kidney and have four types: calcium, uric acid, struvite and cystine, which is a very common urological disease that

karger@karger.com
www.karger.com/kdd

© 2024 The Author(s).
Published by S. Karger AG, Basel

This article is licensed under the Creative Commons Attribution-NonCommercial 4.0 International License (CC BY-NC) (http://www.karger.com/Services/OpenAccessLicense). Usage and distribution for commercial purposes requires written permission.

Correspondence to:
Xiaobo Zhang, zhangxb@csu.edu.cn

affects approximately more than 10% of the global population [1]. Kidney stones may cause severe pain on the lower back, blood urine, fever, and chills and have afflicted mankind for centuries. Importantly, it has been noted that kidney stones are related to an increased risk of severe medical conditions such as cardiovascular disorders [2] and chronic kidney diseases [3]. The treatment for kidney stones, such as nephrolithotripsy, shockwave lithotripsy and percutaneous nephrolithotomy, has made a great progress [4]. However, it is still a serious problem to prevent the recurrence of kidney stones [5]. Therefore, a better understanding of the mechanisms underlying the formation and development of kidney stones is of great importance to the prevention and management of kidney stones.

Neutrophil extracellular traps (NETs) are networks of extracellular chromatin fibers consisting of DNA, histones, and granular proteins [6]. NETs extruded by stimulated neutrophils can entrap and kill invading microbes [7]. In addition, emerging evidence has revealed that NETs are crucial contributors to various diseases [8]. For instance, Yang et al. [9] found that NET formation was increased in the liver metastases of colon and breast cancer patients, and NETs attracted tumor cells to promote cancer metastasis through CCDC25. Nakazawa and colleagues reported that NETs exacerbated renal injury and remote organ dysfunction by releasing histones and cytokines [10]. NETs contribute to gallstone formation [11], but the involvement of NETs in kidney stones remains unknown. A previous study found that neutrophil infiltration and NETs were increased in brushite kidney stones that might promote inflammation in patients [12], suggesting its implication in kidney stones.

Neutrophil elastase (NE), a serine protease enriched in neutrophils, functions as a destructive elastase to destroy the extracellular matrix and regulate inflammation and tissue remodeling [13]. NE degrades histones after its translocation to the nucleus and promotes chromatin decondensation required for NET formation [14]. NE has been linked to inflammatory diseases and chronic kidney and lung disorders [15–17], whereas the role of NET-associated NE in kidney stones has not been reported.

Therefore, the relationship between NETs and kidney stone formation is a mystery. Uncovering the mechanisms by which NETs are involved in kidney stones deepens the understanding of the pathogenesis of kidney stones. Here, we demonstrated that NETs were abundant in patients and rats with kidney stones, and blockade of NETs suppressed the formation and development of kidney stones. Our findings provide novel insights into kidney stone pathogenesis and suggest that targeting NETs may be beneficial to prevent and treat kidney stones.

Materials and Methods

Clinical Specimens

Patients were divided into kidney stone and control groups. In the kidney stone group, 20 patients were diagnosed with kidney stones at Xiangya hospital and received percutaneous nephrolithotomy. In the control group, 20 patients suffered a trauma and received nephrectomy. Control patients did not have medical history of kidney stones, and no urinary tract stone was detected through plain radiography of the kidneys, ureters, and bladder and ultrasonography. Patients with renal failure, chronic diarrhea, urarthritis, medullary sponge kidney, renal tubular acidosis, hypercalcemia, hyperuricemia, hyperparathyroidism, hydronephrosis, urinary system infection, and cancers were excluded from this study. General characteristics of kidney stone and control patients were collected, and no significant difference was observed in general characteristics such as sex ratio and age. Peripheral blood and renal papillary tip tissues were collected from kidney stone and control patients. Blood was centrifugated at 2,000 *g* for 10 min at 4°C for plasma preparation. Renal tissues were fixed in 4% paraformaldehyde solution overnight and processed for paraffin embedding and sectioning at 5 μm. Patients were informed and provided written informed consent. Our study was approved by the Ethics Committee of Xiangya hospital (Approval No. 20210045).

Microarray Data Analysis

We downloaded GSE73680 datasets including papillary tissues from kidney stone patients (n = 56) and patients without kidney stones (n = 6) and from control patients without any kidney stone from Gene Expression Omnibus (https://www.ncbi.nlm.nih.gov/geo/) and analyzed it as previously described. Differentially expressed genes including 270 upregulated genes and 133 downregulated genes were identified using the limma package in R software, and the volcano plot of these genes was generated. Gene ontology (GO) enrichment analysis of differentially expressed genes was conducted using the clusterProfiler package in R software. Furthermore, Kyoto Encyclopedia of Genes and Genomes (KEGG) pathways analysis was performed using Reactome Pathway Database. The protein-protein interaction network of differentially expressed genes was reconstructed through

STRING, and top 10 hub genes, including *CAV1*, *TGFB3*, *FBN1*, *COL4A2*, *COL6A1*, *SERPINH1*, *SPARC*, *MMP1*, *NID1*, and *FN1*, were identified according to the degree score calculated by the cytoHubba plug-in.

Experimental Kidney Stones in Rats

Experimental kidney stones were established as previously described [18]. Male Sprague Dawley rats (8-10-week-old; 200–250 g) were provided by Slake Jingda Laboratory Animal Technology Company (Changsha, Hunan, China) and maintained in a specialized animal facility, which were randomly divided into various groups. In Figures 3 and 4, rats were divided into control and model groups, and rats were divided into PBS, model + PBS and model + Sivelestat (SIVE) groups in Figures 5 and 6. For model groups, to induce kidney stones, rats were administrated with 2 mL of ammonium chloride (1%) and ethylene glycol (1%) through gavage for 4 weeks. Control rats received 2 mL of drinking water. At 0 week (w), 1 w and 4 w, peripheral blood was collected, and rats were sacrificed, and the kidneys were excised for examination of superoxide dismutase (SOD) and malondialdehyde (MDA) and paraffin embedding. Animal procedures were approved by the Ethics Committee of Xiangya hospital (Approval No. 2022020236).

Measurement of NET Biomarkers

The level of cell-free DNA (cf-DNA) in the plasma was determined using Quant-iT™ PicoGreen™ dsDNA Assay Kit (Thermo Fisher Scientific, Waltham, MA, USA) following the manual. Plasma levels of NE, H3Cit, and DNase I were examined using following enzyme-linked immunosorbent assay (ELISA) kits: Rat NE ELISA Kit (Cusabio, Houston, TX, USA), Human NE ELISA Kit (Cusabio), EpiQuik™ Circulating Histone H3 Citrullination ELISA Kit (Epigentek, Farmingdale, NY, USA), Rat DNase I ELISA Kit (LSBio, Seattle, WA, USA), and Human DNase I ELISA Kit (LSBio) according to the manufacturers' recommendations.

Myeloperoxidase-DNA Complex Quantification

The myeloperoxidase (MPO)-DNA complex in the plasma was quantified through ELISA as previous described [19]. Briefly, 96-well plates with high protein binding capacity (Thermo Fisher Scientific) were precoated with a myeloperoxidase polyclonal antibody (Thermo Fisher Scientific) at 5 μg/mL overnight at 4°C. Plates were gently washed, and 100 μL of 2% BSA/PBS solution was added for blocking. The plasma was diluted at 1:10, added into wells and incubated for 2 h. After wash, an anti-DNA HRP antibody (ZYMO RESEARCH, Irvine, CA, USA) was added at 5 μg/mL and incubated for 1 h. TMB substrate (Beyotime, Shanghai, China) was added and incubated for 10 min. The reaction was stopped, and the absorbance at 450 nm was measured.

Immunofluorescence Staining

Paraffin sections were deparaffinized in xylene, rehydrated and processed for heat-induced antigen retrieval in sodium citrate buffer (10 mM; pH 6.0) for 15 min. After natural cooling, sections were washed in water, and sections were permeabilized in 0.5% Triton X-100 solution for 15 min. Then, sections were immersed in 5% normal goat serum for 1 h and incubated with an anti-MPO antibody (1 μg/mL, Abcam, Cambridge, UK), anti-H3Cit antibody (1:20,000, Novus Biologicals, Centennial, CO, USA), or anti-NE antibody (10 μg/mL, Thermo Fisher Scientific) overnight. Subsequently, sections were washed and incubated with an Alexa Fluor 594 or 488-conjugated secondary antibody for 1 h. DAPI (Beyotime) was added to stain nuclei, and sections were mounted and imaged. Images were analyzed and H3Cit+ NE+ positive area was quantified and analyzed using Image J software.

Hematoxylin and Eosin Stain Staining

Paraffin sections were immersed in xylene for dewaxing and rehydrated in gradient concentrations of ethanol and then in water. Subsequently, sections were immersed in hematoxylin solution (beyotime) for 5 min and rinsed in water. Sections were then successively immersed in 95% ethanol for 5 s and in eosin solution for 45 s. After dehydration, sections were cleared in xylene and mounted for observation. Kidney injury was scored: no tubular injury (0), <10% tubular injury (1), <10–25% tubular injury (2), <26–50% tubular injury (3), <51–74% tubular injury (4), and >75% tubular injury (5).

Von Kossa and Periodic Acid-Schiff (PAS) Staining

Von Kossa Stain Kit provided by Abcam was used to stain calcium deposits in paraffin sections. Paraffin sections were dewaxed and rehydrated in distilled water. Sections were immersed in 5% Silver Nitrate Solution and exposed to ultraviolet light for 45 min. After wash, sections were incubated in 5% sodium thiosulfate solution for 2 min and washed in water. Then, sections were stained in nuclear fast red solution for 5 min, washed and dehydrated. Sections were cleared and mounted for observation. The crystal deposition area (black area) was quantified using image J software. For periodic acid-Schiff (PAS) staining, after dewaxing and rehydration, slides were immersed in periodic acid solution for 10 min, washed in water and stained in Schiff's solution for

Table 1. Primer sequences for qRT-PCR

Gene	Forward (5′-3′)	Reverse (5′-3′)
NID1 (human)	AAACACGTTCCAGGCTGTTC	TTGACTGAATGCAACCACGG
FN1 (human)	ACAGGACGGACATCTTTGGT	ATAGGAAGGGGAAGTGGCAC
CAV1 (human)	GCTTCACCACCTTCACTGTG	GCAGGAAAGAGAGAATGGCG
TGFB3 (human)	CGAGTGGCTGTCCTTTGATG	GTCATCCTCATTGTCCACGC
FBN1 (human)	GGACCCCAGTGTGAAAGAGA	CATCTTGACAAGCTCCCGTG
COL4A2 (human)	GGATGAAAGGTGACGATGGC	GGAGTACCCTTCGTTCCAGG
COL6A2 (human)	GCAAGGGGTATCAAGGCAAC	CCTTTGTTGCCAACCTCTCC
SERPINH1(human)	GCCATGTTCTTCAAGCCACA	CTGTCCGGTGCATCATCATG
SPARC (human)	GTTTGAGAAGGTGTGCAGCA	TGTATTTGCAAGGCCCGATG
MMP1 (human)	AAGGTCTCTGAGGGTCAAGC	TCATGAGCTGCAACACGATG
GAPDH (human)	TCGTGGAAGGACTCATGACC	ATGATGTTCTGGAGAGCCCC
NID1 (rat)	AAACACGTTCCAGGCTGTTC	AGGCTCCATTGCTCTTCCAT
FN1 (rat)	TGGGGAATGGAAAAGGGGA	CATTGCATCTGTTCCGGGAG
CAV1 (rat)	CATGGCAGACGAGGTGAATG	TGGTAGACAGCAAGCGGTAA
TGFB3 (rat)	GGAGCCTCTGACCATCTTGT	GGTGAGGTCTGTTGCTTTGG
FBN1 (rat)	TGGAGACCTGCTTCCTCAAG	CTCCCGGCTGTTTCTCAATG
COL4A2 (rat)	CTCGTGGAGCAGAAGGGC	CTCCGAGACTGAGCACCTC
COL6A2 (rat)	CCTGGCTTCAAGGGAGAGAA	ACCTTGGTCTCCTTGCTCTC
SERPINH1 (rat)	ACCCCTTCATCTTCCTGGTG	CCCATGTGTCTCAGGAACCT
SPARC (rat)	GTCCTGGTCACCTTGTACGA	CCAGTGGACAGGGAAGATGT
MMP1 (rat)	TCTGGGTTGTTCGAGAGCAT	CCTGGATCCATGGACTGTGT
GAPDH (rat)	GAGACAGCCGCATCTTCTTG	TGACTGTGCCGTTGAACTTG

qRT-PCR, real-time quantitative reverse transcription PCR.

30 min. After wash, sections were stained with Hematoxylin for 2 min, washed and applied with Bluing reagent for 30 s. Subsequently, slides were incubated with light green solution for 2 min, washed, dehydrated, cleared, and mounted for imaging. PAS stain kit was provided by Abcam. No damage, ≤10%, 11–25%, 26–45%, 46–75%, and ≥76% damage, were represented by grades 0 to 5.

Terminal Deoxynucleotidyl Transferase dUTP Nick-End Labeling Assay

Cell apoptosis in renal tissues was detected by terminal deoxynucleotidyl transferase (TdT) dUTP nick-end labeling (TUNEL) assay using TUNEL assay Kit-HRP-DAB (Abcam) following the manual. Briefly, after dewaxing and rehydration, sections were treated with proteinase K solution for 20 min and washed, and endogenous peroxidases were quenched through incubation in 3% H_2O_2 for 5 min. Sections were washed and equilibrated in TdT Equilibration Buffer for 30 min. Subsequently, TdT labeling reaction mix was applied onto sections, and sections were incubated for 90 min at room temperature. Sections were washed, and the reaction was stopped by adding stop buffer. After 5 min, sections were washed, blocked in blocking buffer and incubated in 1 × conjugate for 30 min. DAB working solution was prepared and applied to sections followed by hematoxylin staining. Five areas surrounding the injury site were randomly selected, and TUNEL-positive cells were quantified and analyzed using Image J software.

Real-Time Quantitative Reverse Transcription PCR

Total RNA was extracted from renal tissues using high pure RNA tissue kit (Sigma-Aldrich, St. Louis, MO, USA) following the manufacturer's recommendation.

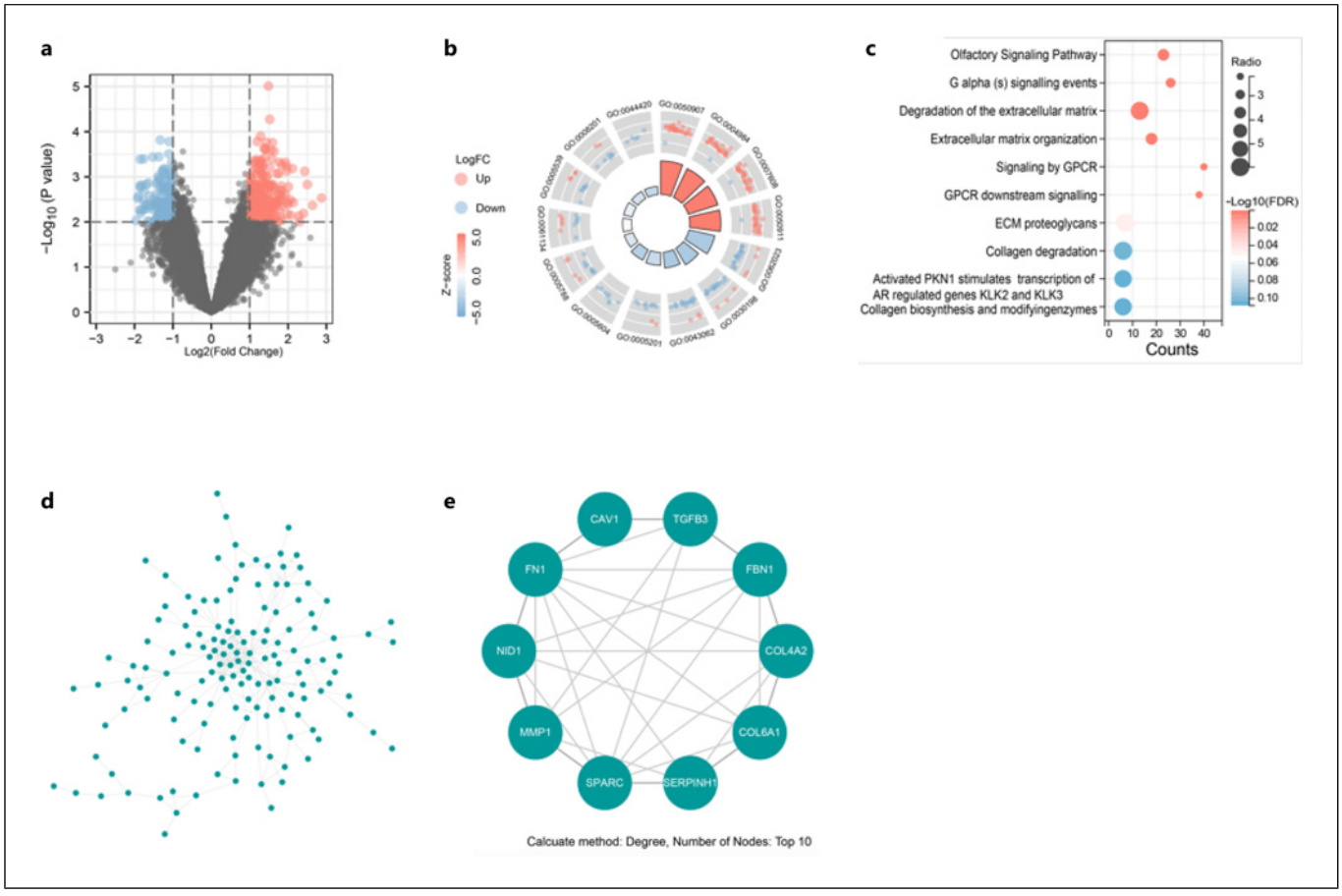

Fig. 1. Dysregulated genes in patients with kidney stones. We analyzed differentially expressed genes in the microarray data from GSE73680. **a** Volcano plot of the microarray data. **b**, **c** GO enrichment and KEGG pathway analysis of differentially expressed genes. **d** PPI network was constructed through STRING. **e** Top ten hub genes were identified via the cytoHubba plug-in. PPI, protein-protein interaction.

RNA quality was examined through electrophoresis and reversely transcribed into cDNA using iScript cDNA Synthesis Kit (Bio-Rad, Hercules, CA, USA). The relative expression of CAV1, TGFB3, FBN1, COL4A2, COL6A1, SERPINH1, SPARC, MMP1, NID1, and FN1 was determined by real-time quantitative PCR. GAPDH was used as a normalization control, and the $2^{-\Delta\Delta Ct}$ method was applied for calculation. Primers are shown in Table 1.

Evaluation of Kidney Oxidative Stress and Biochemical Indicators

SOD activity and MDA content were applied to determine kidney oxidative stress. Rat renal tissues were homogenized in chilled Tris/HCl (0.1 M) containing PMSF (0.1 mg/mL), β-mercaptoethanol (5 mM) and Triton X-100 (0.5%), and tissue extracts were collected after centrifugation at 12,000 *g* for 10 min. SOD activity and MDA content were measured using superoxide dismutase activity assay kit (Sigma-Aldrich) and lipid peroxidation (MDA) assay kit (Sigma-Aldrich) according to the manufacturer's instructions. Plasma levels of creatinine (Cr), blood urea nitrogen (BUN), and calcium were determined with creatinine assay kit (Sigma-Aldrich), urea nitrogen (BUN) colorimetric detection kit (Thermo Fisher Scientific) and calcium assay kit (Abcam), respectively.

Statistical Analysis

Experiment results were from at least three independent assays and presented as mean ± standard deviation. The unpaired *t* test and one-way analysis of variance were applied to analyze the variance of two and multiple groups. $p < 0.05$ was statistically significant.

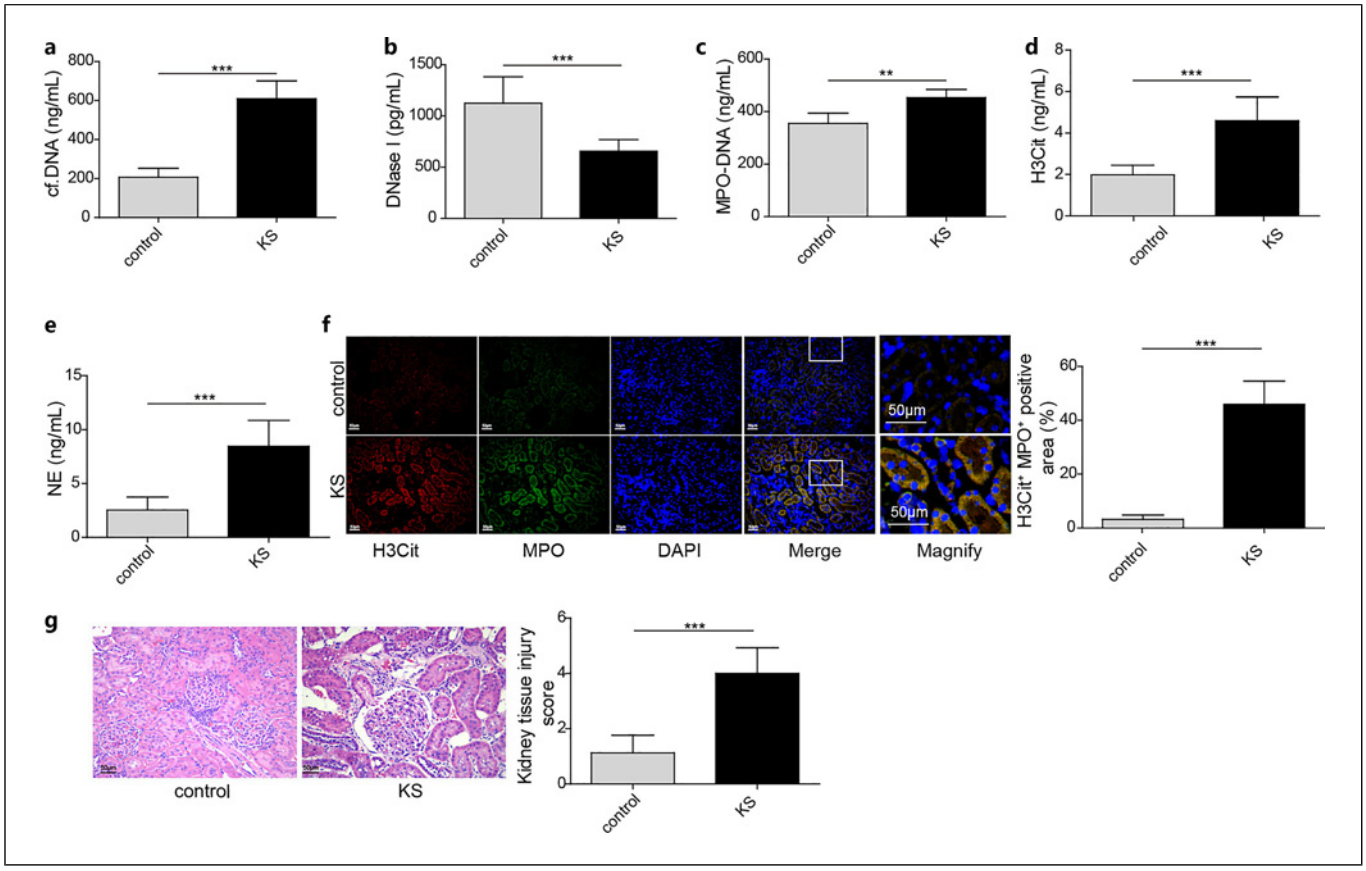

Fig. 2. NETs were elevated in patients with kidney stones. We collected peripheral blood and renal papillary tip tissues from patients with kidney stone and nephrectomy. **a–e** Levels of cf-DNA, DNase I, MPO-DNA, H3Cit, and NE in the plasma (n = 20). **f** IF staining of H3Cit (red) and MPO (green) in renal papillary tip tissues. The nuclei (blue) were stained with DAPI. **g** H&E staining of renal papillary tip tissues. $^{**}p < 0.01$ and $^{***}p < 0.001$. IF, immunofluorescence.

Results

Dysregulated Genes in Patients with Kidney Stones

To explore potential regulators in kidney stones, we analyzed the microarray data from GSE73680, and 403 differentially expressed genes including 270 upregulated and 133 downregulated genes were identified between renal papillary tissues with Randall's plaque and normal papillary tissues (Fig. 1a). Moreover, GO enrichment analysis for biological process terms and KEGG pathway analysis revealed that these differentially expressed genes were tightly associated with olfactory signaling pathway, G alpha (S) signaling events, degradation of the extracellular matrix, extracellular matrix organization, signaling by GPCR, GPCR downstream signaling, ECM proteoglycans and collagen degradation (Fig. 1b, c). Furthermore, we submitted these differentially expressed genes for reconstructing protein-protein interaction network through STRING (Fig. 1d), and top 10 hub genes, including *CAV1*, *TGFB3*, *FBN1*, *COL4A2*, *COL6A1*, *SERPINH1*, *SPARC*, *MMP1*, *NID1*, and *FN1*, were identified according to the degree score calculated by the cytoHubba plug-in (Fig. 1e).

NETs Were Elevated in Patients with Kidney Stones

Given that the above analysis showed that the organization and degradation of the extracellular matrix were involved in kidney stones, and NE, one of the important components of NETs, functions as a destructive elastase to destroy the extracellular matrix [13], our study focused on exploring the role of NETs in kidney stones. NETs consist of NE, MPO, cf-DNA, and histones such as H3Cit, and it is the primary source of circulating cf-DNA [20]. Thus, to identify NETs, we examined levels of cf-DNA, DNase I, MPO-DNA, H3Cit, and NE in the plasma from patients with kidney stones and control patients who

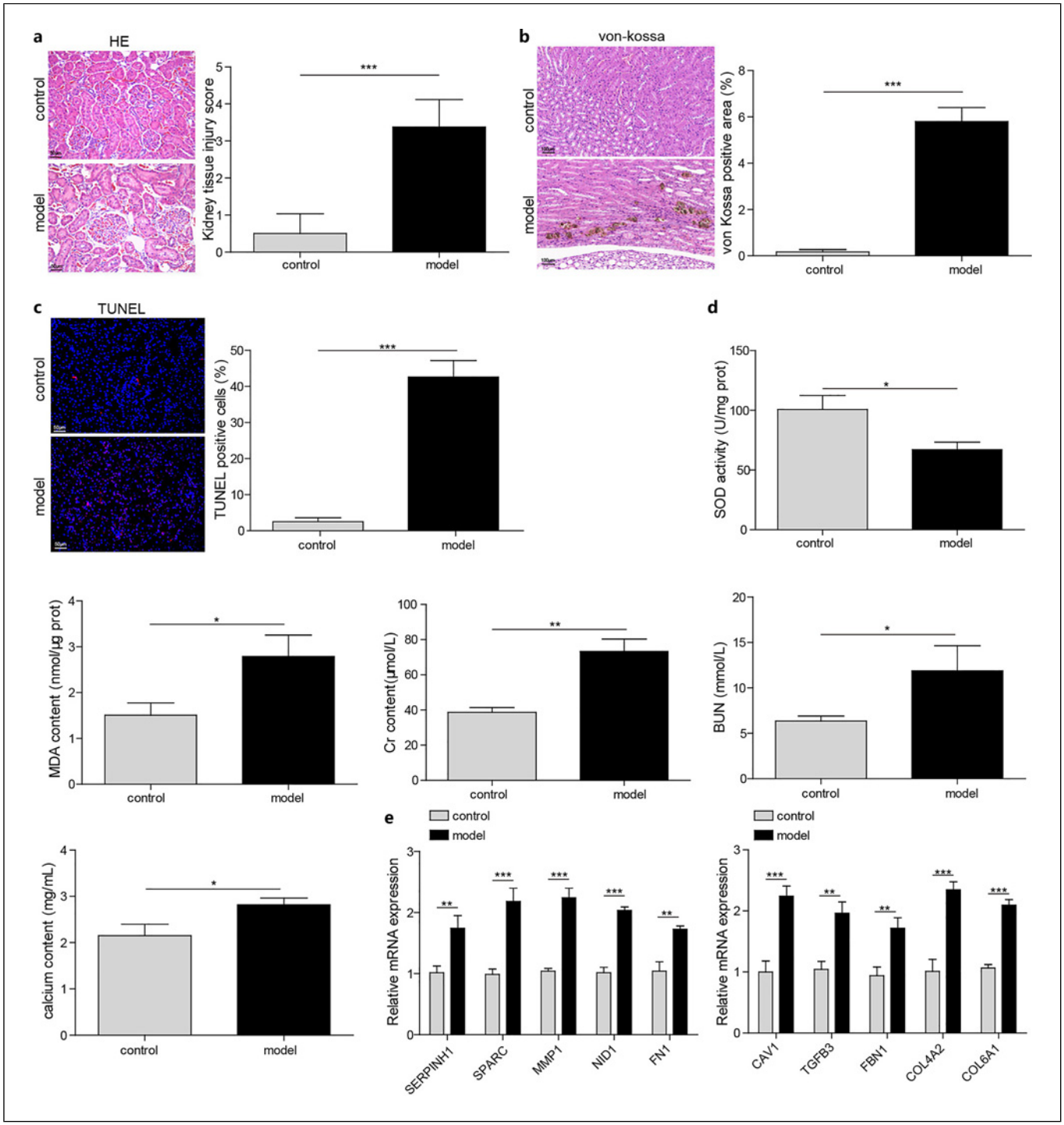

Fig. 3. A rat model of kidney stones was successfully established through ethylene glycol and ammonium chloride administration. Rats were induced with kidney stones and divided into control and model groups. **a** H&E staining for examining renal injury. **b** Von Kossa staining for determining calcium deposits in kidney tissues. **c** TUNEL staining for analyzing cell apoptosis in kidney tissues. **d** SOD activity and MDA in renal tissues and Cr, BUN, calcium in blood were measured ($n = 8$). **e** qRT-PCR analysis of the relative expression of CAV1, TGFB3, FBN1, COL4A2, COL6A1, SERPINH1, SPARC, MMP1, NID1, and FN1. *$p < 0.05$, **$p < 0.01$ and ***$p < 0.001$. qRT-PCR, real-time quantitative reverse transcription PCR.

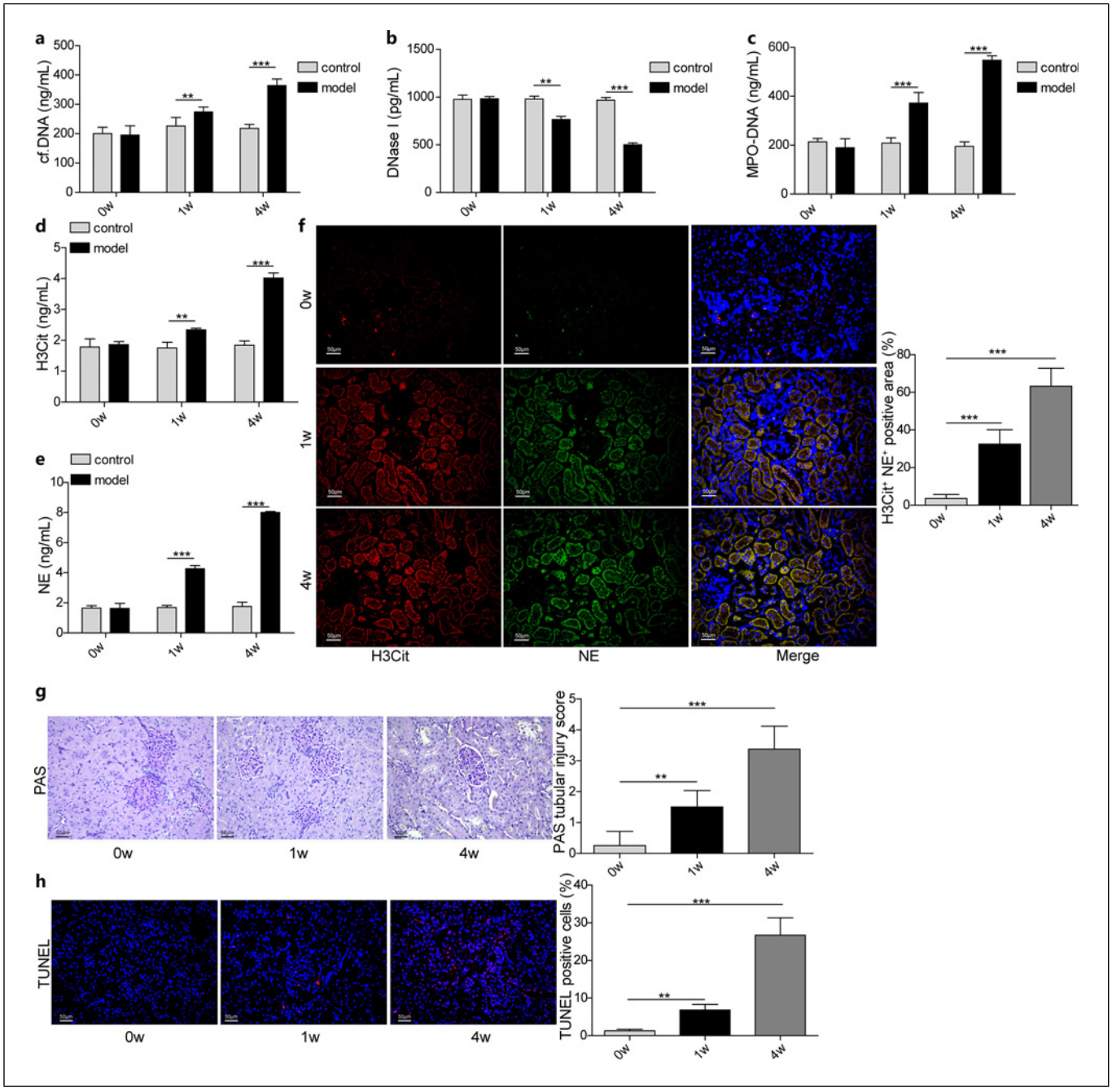

Fig. 4. NET formation was enhanced in rats with experimental kidney stone. Rats were induced with kidney stones at 0 w, 1 w, and 4 w and collected to examine NETs formation. **a–e** Levels of cf-DNA, DNase I, MPO-DNA, H3Cit, and NE in rat plasma at 0 w, 1 w, and 4 w (n = 8). **f** IF staining of H3Cit (red) and NE (green) in renal tissues at 0 w, 1 w, and 4 w. The nuclei (blue) were stained with DAPI. **g** PAS staining for detecting tubular injury at 0 w, 1 w and 4 w. **h** TUNEL staining for analyzing cell apoptosis in kidney tissues at 0 w, 1 w, and 4 w. $^{**}p < 0.01$ and $^{***}p < 0.001$.

suffered a trauma and needed nephrectomy. Increased concentrations of cf-DNA, MPO-DNA, H3Cit, and NE and decreased DNase I level were observed in the plasma from patients with kidney stones compared to control patients (Fig. 2a–e). Moreover, renal papillary tip tissues from patients with kidney stones showed increased

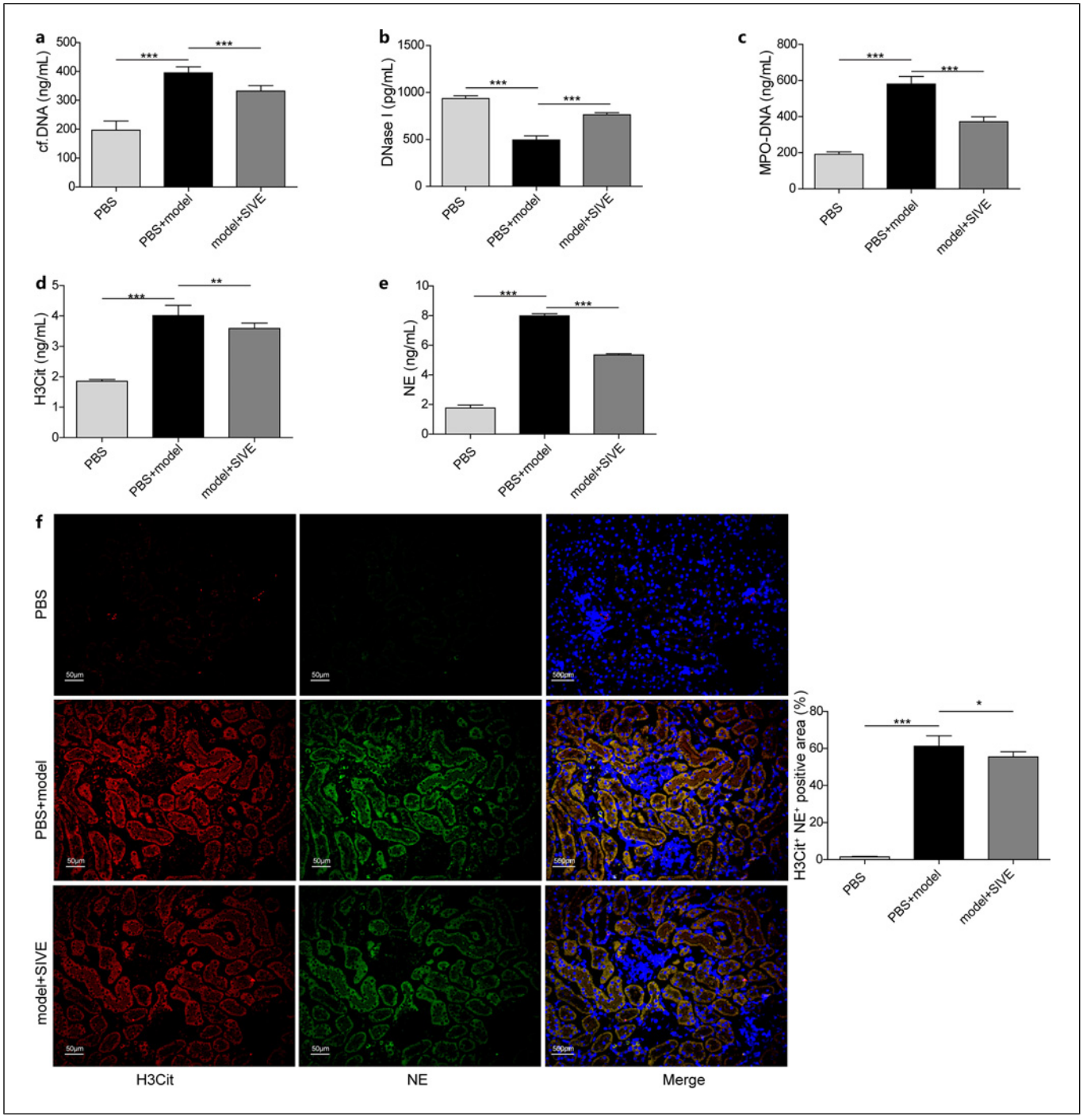

Fig. 5. NETs were inhibited through SIVE administration in rats. Rats with experimental kidney stones were administrated with SIVE to block NETs and divided into three groups: PBS, model + PBS and model + SIVE. **a–e** Levels of cf-DNA, DNase I, MPO-DNA, H3Cit, and NE in rat plasma at 4 w ($n = 8$). **f** IF staining of H3Cit (red) and NE (green) in renal tissues at 4 w. The nuclei (blue) were stained with DAPI. *$p < 0.05$, **$p < 0.01$ and ***$p < 0.001$.

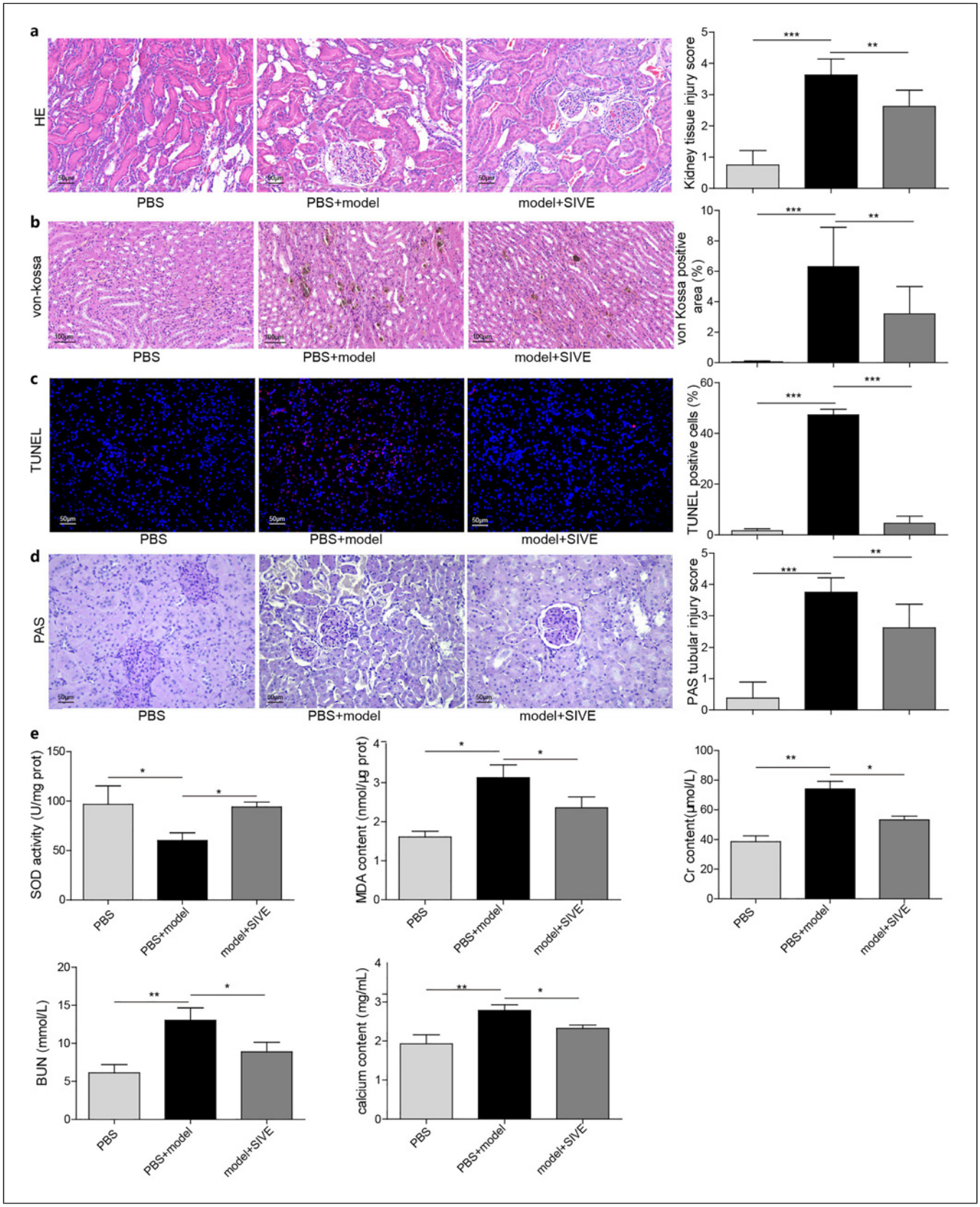

6

(For legend see next page.)

abundance of MPO and H3Cit (Fig. 2f). Hematoxylin and eosin (H&E) staining showed significant pathological renal changes including epithelial cell necrosis, tubular dilation, and mononuclear cell infiltration in patients with kidney stones (Fig. 2g). These results suggested that NET formation was enhanced and might be implicated in kidney stones.

NET Formation Was Enhanced in Experimental Kidney Stone Rats

To evaluate the contribution of NETs to kidney stone formation and development, we established a rat model of kidney stones via gavage administration of ethylene glycol and ammonium chloride. Obvious pathological changes such as tubular dilation and necrosis were observed in the kidneys from experimental rats (Fig. 3a). Von Kossa and TUNEL staining exhibited a significant increase of calcium deposits and cell apoptosis in the kidneys (Fig. 3b, c). In addition, experimental kidney stone rats showed decreased SOD activity and increased MDA content in kidney lysates, and levels of blood Cr, BUN and calcium were increased (Fig. 3d), indicating impaired renal function in kidney stone rats. The top 10 genes identified in Figure 1e were confirmed to be upregulated in the kidneys from kidney stone rats compared to control rats (Fig. 3e). Collectively, these observations demonstrated that the rat model of kidney stones was successfully established. Importantly, we found that levels of cf-DNA, MPO-DNA, H3Cit, and NE were raised and DNase I was reduced in the plasma as kidney stones developed in rats (Fig. 4a–e). In addition, increased abundance of H3Cit and NE revealed that NET formation was enhanced in the kidney with the development of kidney stone in rats (Fig. 4f). As kidney stones developed, tubular injury and cell apoptosis in the kidney were significantly enhanced determined by PAS and TUNEL staining (Fig. 4g, h). Thus, our findings demonstrated the increased presence of NETs in the kidney from experimental kidney stone rats.

Suppression of NETs Ameliorated Nephrolithiasis and Kidney Injury

Furthermore, NETs were suppressed in kidney stone rats via intraperitoneal injection of the NE inhibitor Sivelestat (SIVE) to evaluate whether suppression of NETs regulates kidney stone development. Rats were divided into three groups: PBS, model + PBS and model + SIVE. Elevated levels of cf-DNA, MPO-DNA, H3Cit, and NE and decreased DNase I level were reversed by SIVE administration (Fig. 5a–e). Moreover, increased expression of H3Cit and NE in the kidney from kidney stone rats were inhibited by SIVE (Fig. 5f). These data confirmed that SIVE administration suppressed NET formation in kidney stone rats. H&E staining showed that renal injury was detected in the kidney from rats in the model + PBS group compared to the PBS group, and SIVE obviously reduced renal injury (Fig. 6a). Besides, increased calcium deposits, apoptotic cells, and tubular injury in kidney stone rats were ameliorated by SIVE administration (Fig. 6b–d). SIVE also raised SOD activity and reduced levels of MDA, Cr, BUN, and calcium in kidney stone rats (Fig. 6e), thus improving renal function. In conclusion, suppression of NETs via SIVE could repress the progression of kidney stones.

Discussion

As a common urinary system disorder, kidney stones severely impact patients' health and living quality globally. Kidney stones may lead to severe pain, renal infection, impaired kidney function and hydronephrosis [21, 22], and kidney stone-caused colic is a frequent medical emergency that brings a great burden to the emergency department [23]. The prevalence of kidney stones is steadily growing worldwide, for instance, from 5.95% to 10.63% in the past 30 years in mainland China [24]. Thanks to the development of modern therapies, kidney stones can be treated effectively. Unfortunately, its recurrence rate is extremely high. Almost half of patients relapse in 5–10 years, and the relapse rate in 20 years is approximately 75% [25]. No effective medications are available to prevent its recurrence. Kidney stones are one of the oldest disorders known to medicine, but the mechanisms underlying the formation and development of stones remain largely unknown, even though various factors such as uric acid, renal tubular cell injury and apoptosis, oxidative stress and macromolecules have been found to be important contributors in multiple processes of kidney stone formation [1]. In addition, NETs may induce oxidative stress [26, 27], which may in turn lead to

Fig. 6. Suppression of NETs ameliorated nephrolithiasis and kidney injury. Rats with experimental kidney stones were administrated with SIVE to block NETs and divided into three groups: PBS, model + PBS and model + SIVE. **a** H&E staining of renal tissues at 4 w. **b** Von Kossa staining for determining calcium deposits at 4 w. **c** TUNEL staining for analyzing cell apoptosis at 4 w. **d** PAS staining for detecting tubular injury at 4 w. **e** SOD activity and MDA in renal tissues and Cr, BUN, calcium in blood at 4 w were measured ($n = 8$). *$p < 0.05$, **$p < 0.01$, and ***$p < 0.001$.

accumulation of extracellular matrix proteins [28], suggesting the implication of oxidative stress in kidney stones. Thus, further exploration of the pathogenesis of renal stone formation is vital for the development of novel management and prevention approaches. In the present study, we discovered NETs as a novel mechanism contributing to kidney stones. Specially, we confirmed elevated NET formation in patients with kidney stones, and blockade of NETs restrained experimental kidney stone formation and development in rats, providing the evidence that targeting NETs might be a potential approach for preventing and treating kidney stones.

NETs were firstly uncovered as a mesh-like structure released by hyperactivated neutrophils capable of engulfing and killing invading bacteria in 2004 [7]. Subsequent studies further demonstrated NETs as a key contributor to host defense [29]. Bianchi et al. [30] reported that a specific gene therapy for patients with chronic granulomatous disease endowed antifungal activity and controlled aspergillosis via rebuilding NET formation [30]. On the other hand, emerging evidence has demonstrated that aberrant NETs also show deleterious activities in various pathological conditions. NETs contribute to thrombosis by providing a scaffold and stimulus, linking inflammation and thrombosis [31]. Wong and colleagues found that diabetes enhanced NET formation, and subsequently NETs impaired wound healing in diabetes [32]. In addition, NETs may facilitate tumor metastasis, growth and progression [33]. Moreover, NETs are implicated in various kidney diseases such as lupus nephritis and acute kidney injury [34]. However, its roles in kidney stones have not been reported. Here, we observed increased NET formation in patients with kidney stones and experimental renal stone rats, suggesting a linkage between NETs and the formation and development of kidney stones.

Targeting NETs have shown great potential in treatment of diseases. For instance, suppression of NETs through thrombomodulin could prevent liver metastasis in pancreatic cancer [35]. Adrover et al. [36] discovered that disulfiram mitigated acute lung injury and protected SARS-CoV-2 infection by inhibiting the formation of NETs in rodents. SIVE administration could ameliorate lung damage and endotoxic shock and prevent malaria-related acute lung injury in mice by suppressing NET formation [37, 38]. Therefore, we treated kidney stone rats with SIVE and confirmed that administration of SIVE effectively reduced NET markers, suggesting that SIVE could repress the formation of NETs in rats. Importantly, we demonstrated that blockade of NETs reduced CaOx crystal deposition, apoptotic cells and tubular injury and improved kidney function. Collectively, SIVE-mediated suppression of NETs repressed kidney stones, suggesting that SIVE might be used as an inhibitor of NET for the prevention and treatment of kidney stones.

Conclusion

In summary, we demonstrated that NETs were associated with the processes of kidney stone formation and identified NETs as a vital regulator contributing to the progression of kidney stones. Suppression of NETs via SIVE administration could significantly alleviate kidney stones in rats. Hence, NETs may potentially serve as a therapeutic target, and NET inhibitors such as SIVE and disulfiram may be used for the management of kidney stones. However, the mechanisms by which blockade of NETs restrains kidney stone formation need to be uncovered in future studies.

Statement of Ethics

Patients were informed and provided written informed consent. Our study was approved by the Ethics Committee of Xiangya hospital (Approval No. 20210045). Animal procedures were approved by the Ethics Committee of Xiangya hospital (Approval No. 2022020236).

Conflict of Interest Statement

The authors declare that there is no competing interest.

Funding Sources

This study was supported by National Natural Science Foundation of China (No.82200854).

Author Contributions

Guarantor of integrity of the entire study: X.B.Z.; study design: X.B.Z., Z.M.Y., X.C., and J.G.; literature research: G.N.Q. and X.C.; experimental studies: Z.M.Y., X.B.Z., G.N.Q., X.C., and Z.L.; data analysis and manuscript review: Z.M.Y. and X.B.Z.; statistical analysis: Z.M.Y.; manuscript editing: Z.M.Y. All authors have read and agreed to the published version of the manuscript.

Data Availability Statement

The datasets used or analyzed during this study can be made available from the corresponding author upon reasonable request. The data that support the findings of this study are not publicly available due to their containing information that could compromise the privacy of research participants but are available from X.B.Z.

References

1 Alelign T, Petros B. Kidney stone disease: an update on current concepts. Adv Urol. 2018; 2018:3068365. https://doi.org/10.1155/2018/3068365
2 Rule AD, Roger VL, Melton LJ 3rd, Bergstralh EJ, Li X, Peyser PA, et al. Kidney stones associate with increased risk for myocardial infarction. J Am Soc Nephrol. 2010;21(10): 1641–4. https://doi.org/10.1681/ASN.2010030253
3 Sigurjonsdottir VK, Runolfsdottir HL, Indridason OS, Palsson R, Edvardsson VO. Impact of nephrolithiasis on kidney function. BMC Nephrol. 2015;16:149. https://doi.org/10.1186/s12882-015-0126-1
4 Khan SR, Pearle MS, Robertson WG, Gambaro G, Canales BK, Doizi S, et al. Kidney stones. Nat Rev Dis Primers. 2016; 2:16008. https://doi.org/10.1038/nrdp.2016.8
5 Wang K, Ge J, Han W, Wang D, Zhao Y, Shen Y, et al. Risk factors for kidney stone disease recurrence: a comprehensive meta-analysis. BMC Urol. 2022;22(1):62. https://doi.org/10.1186/s12894-022-01017-4
6 Rada B. Neutrophil extracellular traps. Methods Mol Biol. 2019;1982:517–28. https://doi.org/10.1007/978-1-4939-9424-3_31
7 Brinkmann V, Reichard U, Goosmann C, Fauler B, Uhlemann Y, Weiss DS, et al. Neutrophil extracellular traps kill bacteria. Science. 2004;303(5663):1532–5. https://doi.org/10.1126/science.1092385
8 Mutua V, Gershwin LJ. A review of neutrophil extracellular traps (NETs) in disease: potential anti-NETs therapeutics. Clin Rev Allergy Immunol. 2021;61(2):194–211. https://doi.org/10.1007/s12016-020-08804-7
9 Yang L, Liu Q, Zhang X, Liu X, Zhou B, Chen J, et al. DNA of neutrophil extracellular traps promotes cancer metastasis via CCDC25. Nature. 2020;583(7814):133–8. https://doi.org/10.1038/s41586-020-2394-6
10 Nakazawa D, Kumar SV, Marschner J, Desai J, Holderied A, Rath L, et al. Histones and neutrophil extracellular traps enhance tubular necrosis and remote organ injury in ischemic AKI. J Am Soc Nephrol. 2017;28(6): 1753–68. https://doi.org/10.1681/ASN.2016080925
11 Munoz LE, Boeltz S, Bilyy R, Schauer C, Mahajan A, Widulin N, et al. Neutrophil extracellular traps initiate gallstone formation. Immunity. 2019;51(3):443–50.e4. https://doi.org/10.1016/j.immuni.2019.07.002
12 Makki MS, Winfree S, Lingeman JE, Witzmann FA, Worcester EM, Krambeck AE, et al. A precision medicine approach uncovers a unique signature of neutrophils in patients with brushite kidney stones. Kidney Int Rep. 2020;5(5):663–77. https://doi.org/10.1016/j.ekir.2020.02.1025
13 Polverino E, Rosales-Mayor E, Dale GE, Dembowsky K, Torres A. The role of neutrophil elastase inhibitors in lung diseases. Chest. 2017;152(2):249–62. https://doi.org/10.1016/j.chest.2017.03.056
14 Papayannopoulos V, Metzler KD, Hakkim A, Zychlinsky A. Neutrophil elastase and myeloperoxidase regulate the formation of neutrophil extracellular traps. J Cell Biol. 2010; 191(3):677–91. https://doi.org/10.1083/jcb.201006052
15 Doring G. The role of neutrophil elastase in chronic inflammation. Am J Respir Crit Care Med. 1994;150(6 Pt 2):S114–7. https://doi.org/10.1164/ajrccm/150.6_Pt_2.S114
16 Bronze-da-Rocha E, Santos-Silva A. Neutrophil elastase inhibitors and chronic kidney disease. Int J Biol Sci. 2018;14(10):1343–60. https://doi.org/10.7150/ijbs.26111
17 Voynow JA, Shinbashi M. Neutrophil elastase and chronic lung disease. Biomolecules. 2021; 11(8):1065. https://doi.org/10.3390/biom11081065
18 Yu L, Gan X, Bai Y, An R. CREB1 protects against the renal injury in a rat model of kidney stone disease and calcium oxalate monohydrate crystals-induced injury in NRK-52E cells. Toxicol Appl Pharmacol. 2021;413:115394. https://doi.org/10.1016/j.taap.2021.115394
19 Takeuchi S, Kawakami T, Okano T, Shida H, Nakazawa D, Tomaru U, et al. Elevated myeloperoxidase-DNA complex levels in sera of patients with IgA vasculitis. Pathobiology. 2022;89(1):23–8. https://doi.org/10.1159/000519869
20 Chen XQ, Tu L, Zou JS, Zhu SQ, Zhao YJ, Qin YH. The involvement of neutrophil extracellular traps in disease activity associated with IgA vasculitis. Front Immunol. 2021;12: 668974. https://doi.org/10.3389/fimmu.2021.668974
21 Keddis MT, Rule AD. Nephrolithiasis and loss of kidney function. Curr Opin Nephrol Hypertens. 2013;22(4):390–6. https://doi.org/10.1097/MNH.0b013e32836214b9
22 Nuraj P, Hyseni N. The diagnosis of obstructive hydronephrosis with color Doppler ultrasound. Acta Inform Med. 2017;25(3): 178–81. https://doi.org/10.5455/aim.2017.25.178-181
23 Golzari SE, Soleimanpour H, Rahmani F, Zamani Mehr N, Safari S, Heshmat Y, et al. Therapeutic approaches for renal colic in the emergency department: a review article. Anesth Pain Med. 2014;4(1):e16222. https://doi.org/10.5812/aapm.16222
24 Wang W, Fan J, Huang G, Li J, Zhu X, Tian Y, et al. Prevalence of kidney stones in mainland China: a systematic review. Sci Rep. 2017;7: 41630. https://doi.org/10.1038/srep41630
25 Moe OW. Kidney stones: pathophysiology and medical management. Lancet. 2006; 367(9507):333–44. https://doi.org/10.1016/S0140-6736(06)68071-9
26 Azzouz D, Khan MA, Palaniyar N. ROS induces NETosis by oxidizing DNA and initiating DNA repair. Cell Death Discov. 2021; 7(1):113. https://doi.org/10.1038/s41420-021-00491-3
27 Focken J, Scheurer J, Jager A, Schurch CM, Kamereit S, Riel S, et al. Neutrophil extracellular traps enhance S. aureus skin colonization by oxidative stress induction and downregulation of epidermal barrier genes. Cell Rep. 2023;42(10):113148. https://doi.org/10.1016/j.celrep.2023.113148
28 Verma S, Singh P, Khurana S, Ganguly NK, Kukreti R, Saso L, et al. Implications of oxidative stress in chronic kidney disease: a review on current concepts and therapies. Kidney Res Clin Pract. 2021; 40(2):183–93. https://doi.org/10.23876/j.krcp.20.163
29 Papayannopoulos V. Neutrophil extracellular traps in immunity and disease. Nat Rev Immunol. 2018;18(2):134–47. https://doi.org/10.1038/nri.2017.105
30 Bianchi M, Hakkim A, Brinkmann V, Siler U, Seger RA, Zychlinsky A, et al. Restoration of NET formation by gene therapy in CGD controls aspergillosis. Blood. 2009;114(13): 2619–22. https://doi.org/10.1182/blood-2009-05-221606
31 Fuchs TA, Brill A, Duerschmied D, Schatzberg D, Monestier M, Myers DD Jr, et al. Extracellular DNA traps promote thrombosis. Proc Natl Acad Sci U S A. 2010;107(36): 15880–5. https://doi.org/10.1073/pnas.1005743107
32 Wong SL, Demers M, Martinod K, Gallant M, Wang Y, Goldfine AB, et al. Diabetes primes neutrophils to undergo NETosis, which impairs wound healing. Nat Med. 2015;21(7):815–9. https://doi.org/10.1038/nm.3887
33 Masucci MT, Minopoli M, Del Vecchio S, Carriero MV. The emerging role of neutrophil extracellular traps (NETs) in tumor progression and metastasis. Front Immunol. 2020;11:1749. https://doi.org/10.3389/fimmu.2020.01749
34 Salazar-Gonzalez H, Zepeda-Hernandez A, Melo Z, Saavedra-Mayorga DE, Echavarria R. Neutrophil extracellular traps in the establishment and progression of renal diseases. Medicina. 2019;55(8):431. https://doi.org/10.3390/medicina55080431
35 Kajioka H, Kagawa S, Ito A, Yoshimoto M, Sakamoto S, Kikuchi S, et al. Targeting neutrophil extracellular traps with thrombomodulin prevents pancreatic cancer metastasis. Cancer Lett. 2021;497:1–13. https://doi.org/10.1016/j.canlet.2020.10.015

36 Adrover JM, Carrau L, Dassler-Plenker J, Bram Y, Chandar V, Houghton S, et al. Disulfiram inhibits neutrophil extracellular trap formation and protects rodents from acute lung injury and SARS-CoV-2 infection. JCI Insight. 2022;7(5):e157342. https://doi.org/10.1172/jci.insight.157342

37 Sercundes MK, Ortolan LS, Debone D, Soeiro-Pereira PV, Gomes E, Aitken EH, et al. Targeting neutrophils to prevent malaria-associated acute lung injury/acute respiratory distress syndrome in mice. PLoS Pathog. 2016;12(12):e1006054. https://doi.org/10.1371/journal.ppat.1006054

38 Okeke EB, Louttit C, Fry C, Najafabadi AH, Han K, Nemzek J, et al. Inhibition of neutrophil elastase prevents neutrophil extracellular trap formation and rescues mice from endotoxic shock. Biomaterials. 2020;238:119836. https://doi.org/10.1016/j.biomaterials.2020.119836